Geophysical Research Letters

The Footprint Characteristics of Cosmic Ray Thermal Neutrons

J. Jakobi[1] , J. A. Huisman[1] , M. Köhli[2,3] , D. Rasche[4], H. Vereecken[1] , and H. R. Bogena[1]

[1]Agrosphere Institute (IBG-3), Forschungszentrum Jülich GmbH, Jülich, Germany, [2]Physikalisches Institut, Heidelberg University, Heidelberg, Germany, [3]Physikalisches Institut, University of Bonn, Bonn, Germany, [4]Section Hydrology, German Research Centre for Geosciences, Potsdam, Germany

Abstract The advance of the cosmic ray neutron (CRN) sensing method for estimating field scale soil moisture relied largely on simulations of the footprint properties of epithermal neutrons ($\sim$0.5 eV–100 keV). Commercially available CRN probes are usually additionally equipped with a thermal neutron ($<$0.5 eV) detector. The potential of these measurements is rarely explored because relevant features of thermal neutrons, such as the footprint and the sensitivity to soil moisture are unknown. Here, we used neutron transport modeling and a river crossing experiment to assess the thermal neutron footprint. We found that the horizontal thermal neutron footprint ranges between 43 and 48 m distance from the probe and that the vertical footprint extends to soil depths between 10 and 65 cm depending on soil moisture. Furthermore, we derived weighting functions that quantify the footprint characteristics of thermal neutrons. These results will enable new applications of thermal neutrons.

Plain Language Summary Cosmic ray neutron (CRN) sensing is a method for estimating field-scale soil moisture. It relies on measuring epithermal neutrons above ground. Many CRN detectors allow the measurement of both epithermal and thermal neutrons. However, the thermal neutron data are rarely used because key properties have not been investigated yet. To improve the interpretation of the thermal neutron signal, it is crucial to understand the volume of influence in terms of the areal extent and penetration depth of the soil (i.e., the footprint). We used thermal neutron measurements made while crossing a river with a mobile detector and neutron interaction simulations to assess the footprint of thermal neutrons. Our results showed that 86% of the measured thermal neutrons originate within 43–48 m distance from the CRN detector and from the soil surface down to depths between 10 and 65 cm depending on soil moisture. Furthermore, horizontal and vertical weighting functions were obtained from the simulation results. These findings will enable new applications of thermal neutron detectors, such as the quantification of biomass and snow.

1. Introduction

Cosmic ray neutron (CRN) sensing is a non-invasive method for intermediate scale soil moisture measurements (Zreda et al., 2008). This method relies on the inverse dependence of aboveground epithermal neutrons (energy range from $\sim$0.5 eV to 100 keV) on the environmental hydrogen content in a footprint of 130–240 m radius and soil depths ranging from 15 to 83 cm (Köhli et al., 2015; Schrön et al., 2017). In terrestrial environments, most hydrogen is stored in water in soils. Therefore, it is possible to infer soil moisture content from the amount of aboveground epithermal neutrons. Secondary hydrogen pools, such as biomass, have a large impact on the measurement accuracy, especially when they are not constant in time. For reliable soil moisture estimation, these secondary pools thus need to be considered (Baatz et al., 2014; Bogena et al., 2013; Franz, Zreda, Rosolem, et al., 2013). Recently, it was found that by additionally considering the thermal neutron intensity below $\sim$0.5 eV, aboveground biomass can be inferred using the ratio of thermal to epithermal neutrons (Jakobi et al., 2018; Tian et al., 2016).

CRN sensors are currently installed in approximately 200 locations worldwide (Andreasen et al., 2017). Many of these locations are also instrumented with thermal neutron detectors. However, these extensive data sets are rarely explored because key properties of the thermal neutron signal, such as the footprint of thermal neutrons, are not well defined. Preliminary investigations suggest that the thermal neutron footprint is smaller than the epithermal neutron footprint and in the order of tens of meters (Bogena et al., 2020). For

the improved interpretation of the epithermal neutron signal, horizontal and vertical weighting functions were of great importance. However, such weighting functions are still lacking for thermal neutrons. In addition, the dependence of the thermal neutron footprint on soil moisture and chemical composition is still under debate (e.g., Andreasen et al., 2016; Jakobi et al., 2018; Tian et al., 2016; Zreda et al., 2008).

In this study, we present CRN measurements as well as Monte Carlo simulations using the neutron transport model URANOS (Ultra Rapid Adaptable Neutron-Only Simulations, Köhli et al., 2015). In a first step, we show that URANOS can describe measured thermal neutron fluxes. In a second step, we derive horizontal and vertical weighting functions that describe the thermal neutron footprint from URANOS simulations.

2. Materials and Methods

2.1. River Experiment

According Zreda et al. (2012), coastal transect experiments with mobile CRN detectors are useful to obtain a coarse understanding of CRN footprints and to evaluate neutron intensities simulated with neutron transport models. We measured the changes in neutron intensity along an approximately 1 km long transect with a ferry crossing over the approximately 400 m wide Rhine river near Cologne (central coordinates: 51.056, 6.918) on two days in 2020 (9 September with dry conditions and 21 November with moist conditions). For this, we used the Jülich CRN rover consisting of an array of nine detector units, each holding four $^{10}BF_3$ filled neutron probes (Hydroinnova LLC). Commonly used neutron detectors are far more sensitive to thermal neutrons than to epithermal neutrons. To increase the sensitivity to epithermal neutrons, the detectors are surrounded with high-density polyethylene (HDPE) that moderates a large fraction of the arriving neutrons to lower energy levels. During the experiment we measured neutron intensities with five moderated (with HDPE) and four bare (without HDPE) detector units. To reduce the uncertainty associated to the number of neutron counts (Jakobi et al., 2020), we crossed the river four and six times during the dry and moist conditions, respectively. The maximum driving speed during data acquisition was ∼5 km/h. The time interval between two readings was set to 10 s. In addition to accumulated neutron counts, pressure, humidity and GPS position were recorded. All measurements were assigned to half of the driven distance between two readings. We linearly interpolated hourly incoming neutron counts obtained from the neutron monitor located on the Jungfraujoch (JUNG, available via the NMDB neutron monitor database at www.nmdb.eu) to the measurement times and used these alongside the pressure and humidity measurements to obtain corrected moderated neutron counts. Neutron counts measured with the bare detector were only corrected for pressure and humidity (cf. Jakobi et al., 2018). We also measured soil moisture content in the top 6 cm of the soil on both sides of the river using HydraProbe sensors (Hydra Go Field Version, Stevens Water Monitoring Systems, Inc.). In total, ∼300 measurements were made in dry conditions and ∼200 measurements in moist conditions. Along the measuring transect, different amounts of biomass (i.e., bushes and trees) were present on both sides of the river at distances >∼70 m from the shores.

2.2. Neutron Transport Modeling

We used the URANOS Monte Carlo neutron interaction code for neutron transport modeling (Köhli et al., 2015). The neutron physics of URANOS is based on a ray-casting engine with a voxel geometry. It considers all relevant interaction processes between neutrons and atomic nuclei, such as absorption and evaporation as well as elastic and inelastic collisions in the fast, epithermal and thermal neutron energy regime (Köhli et al., 2015). Several previous neutron modeling studies used simplified approaches where neutrons were launched from within the ground (e.g., Desilets et al., 2010; Zreda et al., 2008) or only secondary neutrons were launched (e.g., Franz, Zreda, Ferré, & Rosolem, 2013; Rosolem et al., 2013). Here, neutrons are launched from a horizontal layer above the soil surface using a realistic energy spectrum (Sato, 2015; Sato & Niita, 2006) for the given geographic location and height above ground (Köhli et al., 2015). The model domain used in this study represents an area of 2,000 × 2,000 m with the source layer having an edge length of 2,600 m and a height that extends from 50 to 80 m. The cutoff rigidity was set to 10 GeV and for each model run, 10^6 source neutrons were simulated. The air medium extended to 1,000 m height and consisted of 78%$_{vol}$ nitrogen, 21%$_{vol}$ oxygen and 1%$_{vol}$ argon at a pressure of 1,020 mbar. The soil extended to 5 m depth and was a homogeneous silica soil consisting of 50%$_{vol}$ solid material, of which 75%$_{vol}$ was SiO_2

and 25%$_{vol}$ Al$_2$O$_3$. The soil bulk density was 1.43 g/cm^3 and the pore space of the soil was filled with H$_2$O and air with the same composition as in the atmosphere. All neutrons that passed a horizontally infinite detector layer between 1.75 and 2 m above ground were recorded if they had prior soil contact. Using a detector layer instead of a dedicated volume detector is equivalent to many detectors located side-by-side (cf. Köhli et al., 2015), and dramatically decreases the number of neutrons that need to be simulated.

2.3. Evaluation of Model Results

Neutrons exhibit different sensitivity and behavior depending on their energy level, which needs to be considered when evaluating neutron modeling results. Here, we consider neutrons ≤0.5 eV and define these as thermal neutrons. This cutoff energy allows for a comparison with earlier modeling results with the Monte Carlo N-Particle Extended (MCNPX) model (e.g., Andreasen et al., 2016, 2020; McJannet et al., 2014).

The kinetic energy of epithermal neutrons decreases monotonically with the number of scattering interactions. In contrast, the kinetic energy of thermal neutrons can increase due to interactions with the environment. Therefore, it is possible that the energy of a thermal neutron increases above 0.5 eV again after the initial thermalization. We do not consider the scattering interactions above 0.5 eV for the presented footprint calculations because we expected different behavior due to their higher energies. Thus, scattering interactions of neutrons with energies above 0.5 eV that subsequently have energies below 0.5 eV are considered as if the energy threshold were never exceeded. If the kinetic energy between two interactions increased by ≥1 eV, we assume that it was absorbed and that a new neutron was released by the target nucleus (i.e., via evaporation).

Following earlier studies describing the epithermal neutron footprint (Desilets & Zreda, 2013; Köhli et al., 2015; Schrön et al., 2017), we define the horizontal footprint (R_{86}) as the lateral distance that 86% of the thermal neutrons traveled from their first soil contact (as thermal neutron) until the passing of the detector layer. The vertical footprint (D_{86}) is defined as 86% of the depth of all scattering interactions in soil that thermal neutrons experienced before passing the detector layer.

3. Results

3.1. River Experiment

Figure 1 shows the results for the measured transect across the Rhine River. On the first measurement day, the soil along the river was significantly drier (red dots; ~0.06 m³/m³) than on the second day (blue dots; ~0.23 m³/m³). As expected, significantly lower neutron intensities were measured on the river compared to the shore areas for both moderated and bare detectors. This difference is less pronounced for moderated detectors than for bare detectors. In addition, the moderated neutrons at the shore showed a clear soil moisture dependence, while the neutrons measured with the bare detectors were less affected by soil moisture.

Figure 1 also shows URANOS simulation results for different soil moisture contents of the shores ranging from 0.10 to 0.50 m³/m³. For this, air humidity (8 g/m³) and air pressure (1,011 mbar) were set to the average conditions during the experiment with dry conditions. The cutoff rigidity was set to 3.15 GeV and obtained from the COSMOS Cutoff Rigidity Calculator (http://cosmos.hwr.arizona.edu/Util/rigidity.php). Neutrons passing the detector layer were accumulated in 50 m distance intervals from the river center. Moderated neutron counts were assumed to constitute of 70% epithermal neutrons (1 eV–1 MeV) and 30% thermal neutrons (McJannet et al., 2014), which is a first order estimate because the actual mixing ratio measured by a moderated detector also contains up to 40% neutrons with energies above 1 MeV and also depends on ambient hydrogen content (Köhli et al., 2018). To consider the energy-dependent sensitivity of the neutron detector, we approximated the neutron counts of a bare detector by weighting the neutrons passing the detector layer with $\sqrt{Energy}^{-1}$ (Weimar et al., 2020). We observed variable amounts of biomass along the driven transect and assumed this to amount to up to 23 kg/m^2. To account for the influence of aboveground biomass (Franz, Zreda, Rosolem, et al., 2013; Jakobi et al., 2018), we reduced the modeled moderated neutron intensities by 0.925% per kg/m^2 (Baatz et al., 2015).
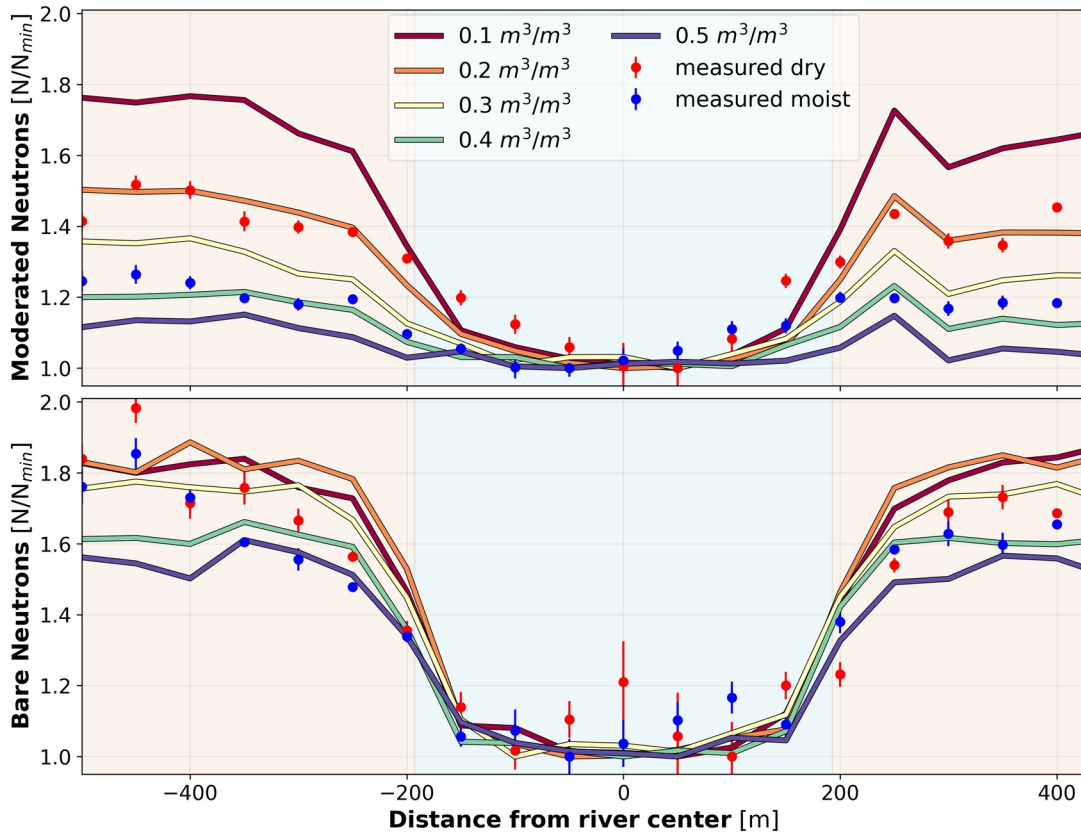
Figure 1. Moderated (upper subplot) and bare (lower subplot) neutron intensity measured (blue and red dots) along an approximately 1 km long transect with the Rhine river in the center (blue zone). In comparison, neutron intensity obtained from Ultra Rapid Adaptable Neutron-Only Simulations (URANOS) for shore soil moistures (orange zones) ranging between 0.10 and 0.50 m³/m³ are shown. For this, moderated neutron intensity was obtained using 70% epithermal neutrons and 30% thermal neutrons. Bare neutron intensity was obtained by weighting neutrons passing the detector layer with $\sqrt{Energy}^{-1}$ (black line in Figure 3a in Weimar et al., 2020).

The URANOS model was able to reproduce reasonably well the trends in both moderated and bare neutron intensity along the transect. A simulated soil moisture of 0.2 m³/m³ provided the best agreement with the measured moderated neutron intensity during the dry experiment, which is higher than the measured value of 0.06 m³/m³ of the upper 6 cm. We attributed this to higher soil moisture at greater depths, resulting in a higher effective soil moisture within the penetration depth of the CRN detector. Similarly, the measured moderated neutron intensity during the wet experiment showed the best agreement with a simulated soil moisture content of 0.40 m³/m³ (measured soil moisture was 0.23 m³/m³ in the upper 6 cm). Both the measured and modeled bare neutron intensities showed stronger gradients than the moderated neutrons near the riverbanks and no clear dependence on soil moisture. The stronger near-shore gradients confirm that the thermal neutron footprint is substantially smaller than the epithermal neutron footprint. However, the footprint cannot be accurately identified with such experimental setups, as it is deformed and biased to drier areas and thus lacks the radial symmetry required to derive a meaningful footprint (Köhli et al., 2015; Schattan et al., 2019). The reasonable agreement between the observed and simulated neutron intensities shows that the relevant physical processes are sufficiently considered in URANOS. Therefore, it will be used to assess the footprint characteristics of thermal neutrons in the following.

3.2. Horizontal Thermal Neutron Footprint

Figure 2 shows the simulated thermal neutron intensity as a function of the radial distance from the first soil contact after thermalization until passing the detector layer for soil moisture contents ranging from 0.06 to 0.50 m³/m³ and for a constant air humidity of 10 g/m³. In addition, Figure 2 shows R_{86} and an analytical
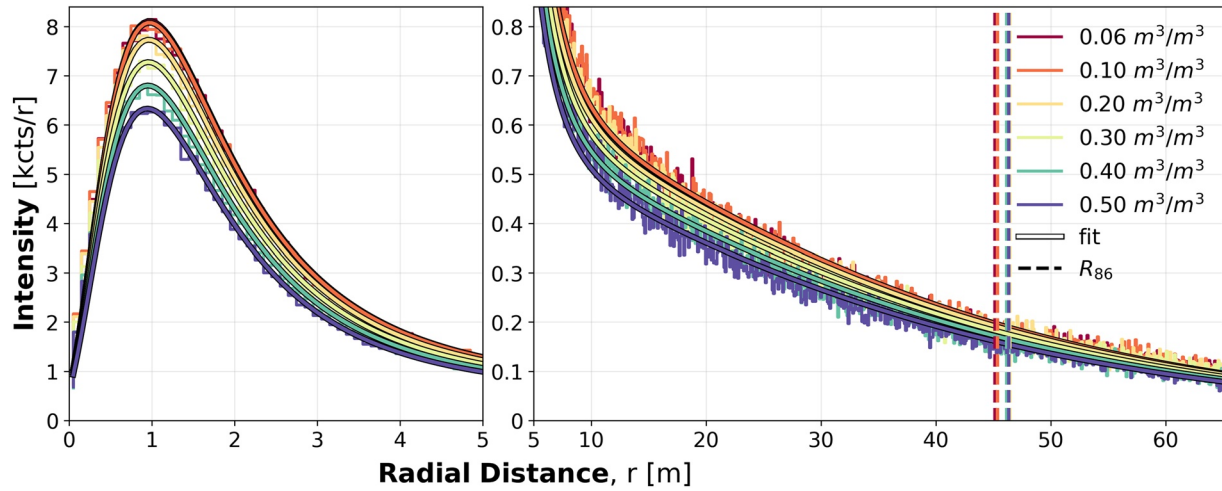
Figure 2. Horizontal intensity of simulated thermal neutrons as a function of distance from the first interaction in the soil to detection for different soil moisture contents ranging from 0.06 to 0.50 m^3/m^3 and constant absolute humidity of 10 g/m^3. The dotted lines indicate the 86% cumulative contribution quantile (R_{86}) for a specific soil moisture content and the solid lines show an analytical fit to the horizontal intensity (W_r — Equation 1).

function that was fitted to the neutron intensity and can be used to obtain the radial weights (W_r, horizontal weighting function):

$$W_r = r^{*F_1}\left(e^{-r^{*F_2}F_3 r^*} + \frac{F_4}{r^*}\right)^{r^* F_5 + F_6}, \quad 0 \leq r^* < 300 \tag{1}$$

where F_1 - F_6 are parametric functions that all depend on soil moisture [m^3/m^3] (see Appendix A). For obtaining r^*, the radial distance from the detector, r in m, can be rescaled for the influence of pressure (p [mbar]) using the approach from Köhli et al. (2015, Equation 5):

$$r^* = r\left(\frac{0.5}{0.86 - e^{-p/1012}}\right)^{-1} \tag{2}$$

However, we suggest to only apply the pressure rescaling to radii > 5 m as we found no evidence that the geometrically controlled peak within the first meters (compare Figure 2) is influenced by air pressure.

We found that more than 45% of the thermal neutrons originated from within 5 m distance from the detector. As in the case of epithermal neutrons (Köhli, 2019), a peak in neutron intensity occurred at these short distances, which is geometrically controlled by the height of the detector above the ground. We also found that the detector height affects R_{86} but not D_{86} (see supporting information). The radial neutron intensity depended on soil moisture and this dependency was more pronounced at shorter distances from the detector. In addition, R_{86} increased slightly with increasing soil moisture. Within the considered soil moisture and air humidity range from 0.01 to 0.50 m^3/m^3 and 1 to 21 g/m^3, R_{86} ranged between 43 and 48 m. In contrast to the strong dependence of the epithermal neutron footprint on air humidity (Köhli et al., 2015), an increase in air humidity from 1 to 21 g/m^3 for a soil moisture of 0.20 m^3/m^3 only resulted in a decrease in R_{86} of thermal neutrons by ∼2 m. This weak dependence on air humidity can be explained by the shorter travel paths of thermal neutrons and the associated lower probability of interaction with water vapor nuclei compared to epithermal neutrons (Desilets & Zreda, 2013). Because of this weak dependence, we did not consider air humidity as a parameter in Equation 1.

3.3. Vertical Thermal Neutron Footprint

Figure 3 shows the contribution of scattering interactions of detected thermal neutrons as a function of depth in the soil for soil moisture contents ranging from 0.06 to 0.50 m^3/m^3 with a constant air humidity of 10 g/m^3 and for various distances from the detector. Furthermore, Figure 3 shows D_{86} (i.e., the penetration depth) and the fitted analytical function (W_d, vertical weighting function):
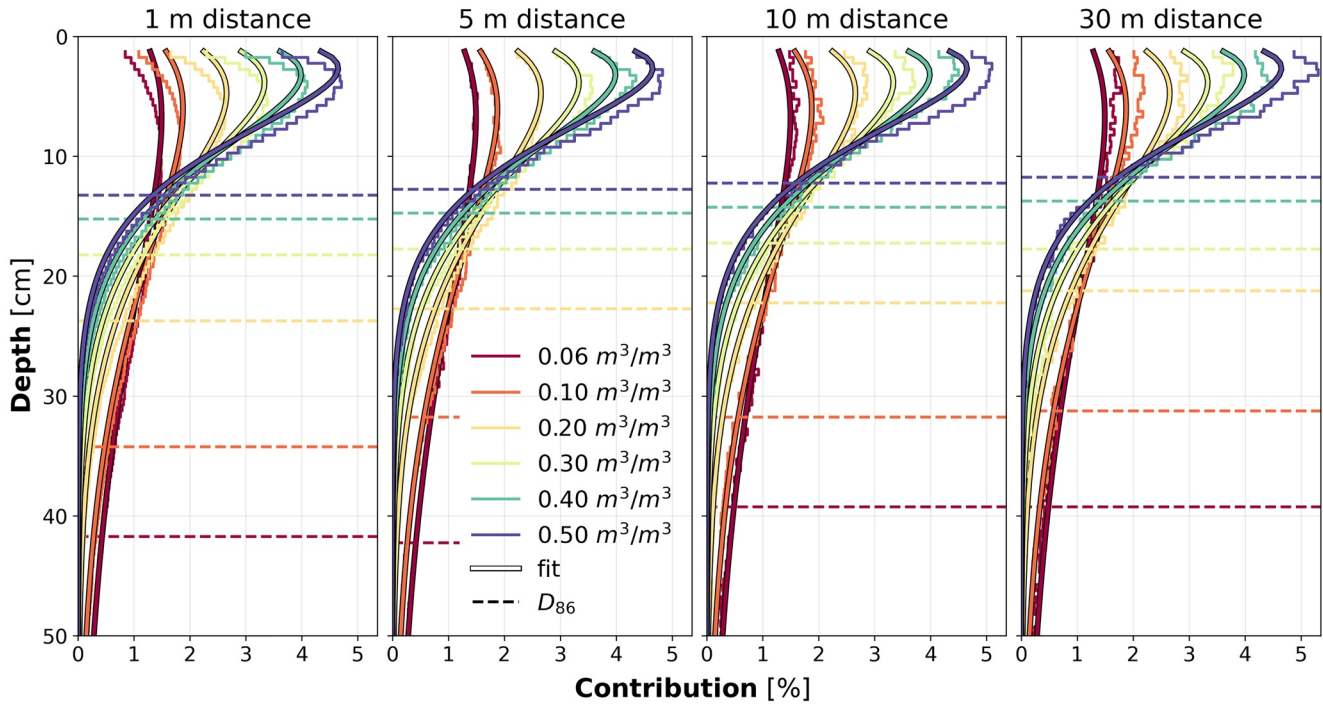
Figure 3. Vertical contribution of all scattering interactions of thermal neutrons to the total neutron flux at 1, 5, 10, and 30 m distance from the first interaction in the soil to detection for different soil moisture contents ranging from 0.06 to 0.50 m^3/m^3 and constant absolute humidity of 10 g/m^3. The dotted lines indicate the 86% cumulative contribution quantile (D_{86}) for a specific soil moisture content and the solid lines show an analytical fit to the vertical contribution (W_d—Equation 3).

$$W_d = d^{F_7}\left(e^{-d^{F_8}F_9 d} + \frac{F_{10}}{d}\right)^{dF_{11}+F_{12}}, \quad 1 \le d \le 150 \tag{3}$$

where F_7 - F_{12} are parameter functions dependent on soil moisture [m^3/m^3] (see Appendix A) and d in cm is the soil depth.

The simulations for the vertical thermal neutron footprint indicate that the penetration depth decreases from 65 to 10 cm with increasing soil moisture from 0.01 to 0.50 m^3/m^3 (not all shown) and decreases slightly with increasing radial distance (Figure 3). Compared to epithermal neutrons, the radial decrease of D_{86} with distance was far less pronounced for thermal neutrons (cf. Köhli et al., 2015; Schrön et al., 2017). Figure 3 also shows a strong dependence on soil moisture for the contribution of the scattering interactions to the overall measured signal. For short distances (i.e., at ~1 m distance), the normalized contribution to the overall signal in the soil strongly varied within the first centimeters. In contrast, the vertical weights of epithermal neutrons decrease monotonous (Franz et al., 2012; Köhli et al., 2015; Schrön et al., 2017). There was only a small radial dependence of the vertical contribution. Therefore, this was not considered in the vertical weighting function (Equation 3). The best agreement between the modeled contribution to the total signal and W_d obtained from Equation 3 was found at ~5 m distance from the detector (Figure 3). Considering that soil moisture measurements for calibration are usually generated from mixed samples in 5 cm intervals (e.g., Zreda et al., 2012; Scheiffele et al., 2020) or from distributed sensor networks with the first measurement in a soil depth of ~5 cm (e.g., Bogena et al., 2013), the weighing function fits the simulation results well enough for practical applications.

4. Discussion

The footprint definitions used in this study have shown good results for the weighting of reference soil moisture measurements in many experimental studies with epithermal neutrons (e.g., Bogena et al., 2020; Scheiffele et al., 2020; Schrön et al., 2017). We therefore expect that these definitions are also appropriate for thermal neutrons. Furthermore, the use of the same definitions allows for easier comparison with previous work. Nonetheless, it is worth mentioning two issues with the used definitions for the thermal neutron footprint. First, the use of 86% quantiles to summarize the footprint characteristics provides a favorable impression of the size of the footprint. In reality, a large fraction of both epithermal and thermal neutrons is expected to originate from a region close to the detector (Köhli et al., 2015, Figure 2). Second, the use of the first soil contact of a neutron to determine the horizontal intensity and all scattering interactions to determine the vertical contribution is a simplification that not necessarily represents the neutron signal measured by the detector. In future studies, an attempt should be made to formulate the definitions for the lateral and vertical footprint more consistently.

In our opinion, defining the origin of a thermal neutron by its first soil contact with kinetic energies ≤0.5 eV is a meaningful choice, because this is in proximity to the kinetic energy ($\sim$0.17 eV) where the dominant physical response of neutrons changes from elastic scattering interactions to absorption (cf. Köhli et al., 2018; Weimar et al., 2020). Nevertheless, it is unclear to which extent the sensitivity of thermal neutrons to soil moisture depends on soil interactions with higher energies before a neutron is moderated down to thermal energies. Thus, defining the first soil contact as thermal neutron as origin may provide biased results.

The density of aboveground thermal neutrons not only depends on the rate of higher energy neutrons that are thermalized, but also on the absorption by nuclei mainly in soils (Desilets et al., 2010; Zreda et al., 2008). For instance, Andreasen et al. (2016) found that the gadolinium concentration in soils needed to be considered to simulate realistic thermal neutron intensities. In this study, we did not explicitly consider the effect of modified soil chemistry on the footprint properties of thermal neutrons. However, we found only a reduction in R_{86} by $\sim$2 m and a reduction in D_{86} by $\sim$5 cm when adding 10^{-6} g/cm^3 ^{10}B to the soil in the model domain (for a soil moisture of 0.20 m^3/m^3). This ^{10}B content approximately represents the cumulative absorption cross section (Sears, 1992) of the European median amounts of the most important soil elements (Salminen et al., 2005). Consequently, we assume that the influence of soil chemistry on the thermal neutron footprint is small in most cases.

Standard neutron detectors that use HDPE for moderation typically show a contribution of $\sim$20%–30% thermal neutrons to the moderated signal (Köhli et al., 2018; McJannet et al., 2014). Similarly, epithermal neutrons also influence the signal of a bare detector, but to a lesser degree (Andreasen et al., 2016). For future studies, it would be important to investigate the contribution of thermal and epithermal neutrons to the moderated and bare neutron detectors in more detail. This would allow a complementary use of the weighting schemes from Schrön et al. (2017) for epithermal neutrons and the weighting scheme (Equations 1–3) proposed in this study for thermal neutrons to more accurately describe the total measured neutron signals of moderated and bare detectors.

5. Conclusions and Outlook

This study presents for the first time a detailed assessment of the thermal neutron footprint of cosmic ray neutrons using the neutron transport model URANOS. Our neutron transport simulations showed that the horizontal footprint of thermal neutrons (≤0.5 eV) depends only slightly on soil moisture and ranges between 43 to 48 m for soil moisture contents between 0.01 and 0.50 m^3/m^3. In contrast, we found that the penetration depth of thermal neutrons strongly depends on soil moisture and ranges from 10 to 65 cm for soil moisture contents between 0.01 and 0.50 m^3/m^3. Furthermore, we found a low influence of air humidity on the footprint of thermal neutrons. In addition, we measured neutron intensity along a transect that crossed a river using a highly sensitive cosmic-ray rover. Since the URANOS neutron transport model was able to adequately reproduce the measured bare neutron intensities of the transect across the river, we are confident that it is suitable for the thermal neutron footprint simulations presented here. Our results should enable new applications using thermal neutrons, such as the improved correction of biomass for soil moisture determination or the detection of biomass changes. For future studies, we suggest to investigate the

dependence of the thermal neutron footprint on soil chemistry, vegetation, detector height above ground and soil bulk density in more detail. In addition, future research should investigate the contributions of epithermal and thermal neutrons to the measured signals of different types of bare and moderated detectors. Furthermore, the applicability of the pressure, air humidity and incoming cosmic ray neutron standard correction models for thermal neutrons should be investigated.

Appendix A

The parameter functions F_i all depend on soil moisture (θ [m^3/m^3]) and can be subdivided into a set of linear functions (Equation A1) and a set of power functions (Equation A2):

$$F_1, F_2, F_3, F_6, F_8, F_9 = p_1\theta + p_2 \tag{A1}$$

$$F_4, F_5, F_7, F_{10}, F_{11}, F_{12} = p_1\theta^{p_2} \tag{A2}$$

The parameters that apply to the functions F_i are provided in Table A1.

Table A1
Parameters for the Functions F_i

Parameter-function	p_1	p_2
F_1	−1.90331	18.33714
F_2	0.03771	−0.34645
F_3	−0.04252	1.55665
F_4	1.44161	0.00355
F_5	0.00767	−0.01029
F_6	−1.86707	18.32828
F_7	−164.3489	0.12357
F_8	−0.107	−0.79174
F_9	0.49036	5.19522
F_{10}	1.01168	−0.00738
F_{11}	0.10415	0.79743
F_{12}	−164.80664	0.12448

Conflict of Interest

Markus Köhli is the CEO of Styx Neutronica, a company building cosmic ray neutron probes.

Data Availability Statement

The rover data sets used in this study can be accessed through the TERENO (Terrestrial Environmental Observatories) Geoportal at https://doi.org/10.34731/1dg7-3x98%20.

References

Andreasen, M., Jensen, K. H., Bogena, H., Desilets, D., Zreda, M., & Looms, M. C. (2020). Cosmic ray neutron soil moisture estimation using physically based site—Specific conversion functions. *Water Resources Research*, *56*, e2019WR026588. https://doi.org/10.1029/2019WR026588

Andreasen, M., Jensen, K. H., Desilets, D., Franz, T., Zreda, M., Bogena, H. R., & Looms, M. C. (2017). Status and perspectives of the cosmic-ray neutron method for soil moisture estimation and other environmental science applications. *Vadose Zone Journal*, *16*, 4079. https://doi.org/10.2136/vzj2017.04.0086

Andreasen, M., Jensen, K. H., Zreda, M., Desilets, D., Bogena, H. R., & Looms, M. C. (2016). Modeling cosmic-ray neutron field measurements. *Water Resources Research*, *52*, 6451–6471. https://doi.org/10.1002/2015WR018236

Baatz, R., Bogena, H. R., Hendricks Franssen, H.-J., Huisman, J. A., Montzka, C., & Vereecken, H. (2015). An empirical vegetation correction for soil water content quantification using cosmic ray probes. *Water Resources Research*, *51*, 2030–2046. https://doi.org/10.1002/2014WR016443

Baatz, R., Bogena, H. R., Hendricks Franssen, H.-J., Huisman, J. A., Qu, W., Montzka, C., & Vereecken, H. (2014). Calibration of a catchment scale cosmic-ray probe network: A comparison of three parametrization methods. *Journal of Hydrology*, *516*, 231–244. https://doi.org/10.1016/j.jhydrol.2014.02.026

Bogena, H. R., Herrmann, F., Jakobi, J., Brogi, C., Ilias, A., Huisman, J. A., et al. (2020). Monitoring of snowpack dynamics with cosmic-ray neutron probes: A comparison of four conversion methods. *Frontiers in Water*, *2*, 19. https://doi.org/10.3389/frwa.2020.00019

Bogena, H. R., Huisman, J. A., Baatz, R., Hendricks Franssen, H.-J., & Vereecken, H. (2013). Accuracy of the cosmic-ray soil water content probe in humid forest ecosystems: The worst case scenario. *Water Resources Research*, *49*, 5778–5791. https://doi.org/10.1002/wrcr.20463

Desilets, D., & Zreda, M. (2013). Footprint diameter for a cosmic-ray soil moisture probe: Theory and Monte Carlo simulations. *Water Resources Research*, *49*, 3566–3575. https://doi.org/10.1002/wrcr.20187

Desilets, D., Zreda, M., & Ferré, T. P. A. (2010). Nature's neutron probe: Land surface hydrology at an elusive scale with cosmic rays. *Water Resources Research*, *46*, W11505. https://doi.org/10.1029/2009WR008726

Franz, T. E., Zreda, M., Ferré, T. P. A., & Rosolem, R. (2013). An assessment of the effect of horizontal soil moisture heterogeneity on the area-average measurement of cosmic-ray neutrons. *Water Resources Research*, *49*, 6450–6458. https://doi.org/10.1002/wrcr.20530

Franz, T. E., Zreda, M., Ferré, T. P. A., Rosolem, R., Zweck, C., Stillman, S., et al. (2012). Measurement depth of the cosmic ray soil moisture probe affected by hydrogen from various sources. *Water Resources Research*, *48*, W08515. https://doi.org/10.1029/2012WR011871

Franz, T. E., Zreda, M., Rosolem, R., Hornbuckle, B. K., Irvin, S. L., Adams, H., et al. (2013). Ecosystem-scale measurements of biomass water using cosmic ray neutrons. *Geophysical Research Letters*, *40*, 3929–3933. https://doi.org/10.1002/grl.50791

Jakobi, J., Huisman, J. A., Schrön, M., Fiedler, J., Brogi, C., Vereecken, H., & Bogena, H. R. (2020). Error estimation for soil moisture measurements with cosmic ray neutron sensing and implications for rover surveys. *Frontiers in Water*, *2*(10). https://doi.org/10.3389/frwa.2020.00010

Jakobi, J., Huisman, J. A., Vereecken, H., Diekkrüger, B., & Bogena, H. R. (2018). Cosmic ray neutron sensing for simultaneous soil water content and biomass quantication in drought conditions. *Water Resources Research*, *54*, 7383–7402. https://doi.org/10.1029/2018WR022692

Köhli, M. (2019). *The CASCADE 10B thermal neutron detector and soil moisture sensing by cosmic-ray neutrons*. (Doctoral thesis). Heidelberg, Germany: Physikalisches Institut, Heidelberg University.

Köhli, M., Schrön, M., & Schmidt, U. (2018). Response functions for detectors in cosmic ray neutron sensing. *Nuclear Instruments Methods in Physics Research Section A: Accelerators, Spectrometers, Detectors and Associated Equipment*, *902*, 184–189. https://doi.org/10.1016/j.nima.2018.06.052

Köhli, M., Schrön, M., Zreda, M., Schmidt, U., Dietrich, P., & Zacharias, S. (2015). Footprint characteristics revised for eld-scale soil moisture monitoring with cosmic-ray neutrons. *Water Resources Research*, *51*, 5772–5790. https://doi.org/10.1002/2015WR017169

McJannet, D., Franz, T., Hawdon, A., Boadle, D., Baker, B., Almeida, A., et al. (2014). Field testing of the universal calibration function for determination of soil moisture with cosmic-ray neutrons. *Water Resources Research*, *50*, 5235–5248. https://doi.org/10.1002/2014WR015513

Rosolem, R., Shuttleworth, W. J., Zreda, M., Franz, T. E., Zeng, X., & Kurc, S. A. (2013). The effect of atmospheric water vapor on neutron count in the cosmic-ray soil moisture observing system. *Journal of Hydrometeorology*, *14*(5), 1659–1671. https://doi.org/10.1175/JHM-D-12-0120.1

Salminen, R., Batista, M. J., Bidovec, M., Demetriades, A., De Vivo, B., De Vos, W., et al. (2005). *FOREGS geochemical atlas of Europe. Part 1 – Background information and maps*. http://weppi.gtk.fi/publ/foregsatlas/

Sato, T. (2015). Analytical model for estimating terrestrial cosmic ray fluxes nearly anytime and anywhere in the world: Extension of PARMA/EXPACS. *PloS One*, *10*, e0144679. https://doi.org/10.1371/journal.pone.0144679

Sato, T., & Niita, K. (2006). Analytical functions to predict cosmic-ray neutron spectra in the atmosphere. *Radiation Research*, *166*(3), 544–555. https://doi.org/10.1667/RR0610.1

Schattan, P., Köhli, M., Schrön, M., Baroni, G., & Oswald, S. E. (2019). Sensing area-average snow water equivalent with cosmic-ray neutrons: The influence of fractional snow cover. *Water Resources Research*, *55*, 10796–10812. https://doi.org/10.1029/2019WR025647

Scheiffele, L., Baroni, G., Frant, T. E., Jakobi, J., & Oswald, E. S. (2020). A profile shape correction to reduce the vertical sensitivity of cosmic-ray neutron sensing of soil moisture. *Vadose Zone Journal*, *19*, e20083. https://doi.org/10.1002/vzj2.20083

Schrön, M., Köhli, M., Scheiffele, L., Iwema, J., Bogena, H. R., Lv, L., et al. (2017). Improving calibration and validation of cosmic-ray neutron sensors in the light of spatial sensitivity — Theory and evidence. *Hydrology and Earth System Sciences*, *21*, 5009–5030. https://doi.org/10.5194/hess-21-5009-2017

Sears, V. F. (1992). Neutron scattering lengths and cross sections. *Neutron News*, *3*(3), 26–37. https://doi.org/10.1080/10448639208218770

Tian, Z. C., Li, Z. Z., Liu, G., Li, B. G., & Ren, T. S. (2016). Soil water content determination with cosmic-ray neutron sensor: Correcting aboveground hydrogen effects with thermal/fast neutron ratio. *Journal of Hydrology*, *540*, 923–933. https://doi.org/10.1016/j.jhydrol.2016.07.004

Weimar, J., Köhli, M., Budach, C., & Schmidt, U. (2020). Large-scale boron-lined neutron detection systems as a [3]He alternative for cosmic ray neutron sensing. *Frontiers in Water*, *2*(16). https://doi.org/10.3389/frwa.2020.00016

Zreda, M., Desilets, D., Ferré, T. P. A., & Scott, R. L. (2008). Measuring soil moisture content non-invasively at intermediate spatial scale using cosmic-ray neutrons. *Geophysical Research Letters*, *35*, L21402. https://doi.org/10.1029/2008GL035655

Zreda, M., Shuttleworth, W. J., Xeng, X., Zweck, C., Desilets, D., Franz, T. E., et al. (2012). COSMOS: The Cosmic-ray soil moisture observing system. *Hydrology and Earth System Sciences*, *16*(1), 1–18. https://doi.org/10.5194/hess-16-1-201210.5194/hess-16-4079-2012